Article

In-Situ High-Temperature Studies of Diblock Copolymer Structural Evolution

Nataliya A. Yufa, Jason Li, and S. J. Sibener

Macromolecules, **2009**, 42 (7), 2667-2671• DOI: 10.1021/ma802751c • Publication Date (Web): 09 March 2009

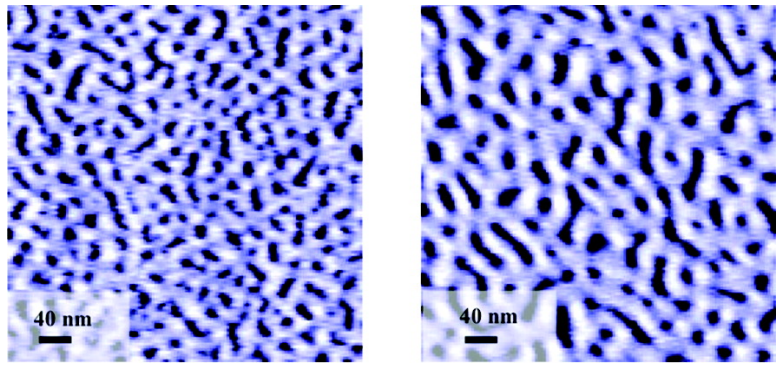

In-Situ High-Temperature Studies of Diblock Copolymer Structural Evolution

Nataliya A. Yufa,[†] Jason Li,[‡] and S. J. Sibener*[,§]

James Franck Institute and Department of Physics, University of Chicago, Chicago, Illinois 60637; Asylum Research Corporation, Santa Barbara, California 93117; and James Franck Institute and Department of Chemistry, University of Chicago, Chicago, Illinois 60637

Received December 9, 2008; Revised Manuscript Received February 9, 2009

ABSTRACT: We present the results of imaging cylinder-forming poly(styrene-*block*-methyl methacrylate) diblock copolymer at temperatures high enough to show polymer domains evolving. Atomic force microscopy movies of morphological polymer evolution are analyzed to shed light on the formation of domains as well as the mechanism which drives their subsequent development, such as spatial domain wall fluctuations.

Introduction

Diblock copolymers are a promising class of materials due to their ability to self-assemble into a variety of morphologies on the nanoscale.[1−5] They have been used to create well-ordered arrays[6] and more recently as lithographic templates[7] and scaffolds for magnetic hard drives.[8] For most applications, long-range order is crucial. Because it presents both blocks at the free surface in ultrathin films, poly(styrene-*block*-methyl methacrylate) (PS-*b*-PMMA) is an excellent model system to study in situ the processes that lead to the creation of order. Since no etching is necessary to reveal both the majority and minority block, this polymer can be imaged with atomic force microscopy (AFM) and its evolution observed directly.[9] This is particularly advantageous as it allows variable-temperature AFM imaging to probe the real-time and real-space dynamics of the PS-*b*-PMMA sample used in this study[10] in the thermal region which encompasses the glass transition temperature, T_g.

Many rheological, as well as small-angle neutron and X-ray scattering investigations have been performed on the structural evolution of thin polymer films.[11−14] These studies have shown the collective behavior of various block copolymers, such as changes in spatial periodicity and bulk moduli as a function of time or temperature. In this study we have observed the real-space behavior of hundreds of individual domains—something which could not be accomplished with rheological or scattering methods.

There have been prior high-temperature AFM studies, which have probed, for example, the micron-scale behavior of thin films during microphase separation as well the phase behavior of block copolymer at a fixed temperature.[15,16] Here we report findings on the process of formation of microdomains as the samples are heated above the glass transition temperature T_g as well as our observations regarding polymer behavior as a function of temperature. To our knowledge, the work presented herein is the first such study on the nanoscale.

There is a great deal of interest in determining the exact mechanism responsible for microphase separation and polymer evolution in block copolymers.[17−20] The main theories include large-scale flows,[21] domain curvature minimization,[22] tube-like reptation,[23] and Rousian diffusion.[24] By compiling our still AFM images into time-lapse movies, we have been able to observe how small-scale fluctuations result in domain joints and separations.

Previously, Magerle and colleagues have examined diblock copolymer evolution in a narrow temperature range above T_g.[16] Our setup allowed us to take data at a range of temperatures, both below and above T_g. We were, therefore, able to compare diblock copolymer behavior at different temperatures.

Experimental Procedure

We used syndiotactic 77 000 g/mol PS-*b*-PMMA (55K PS−22K PMMA) obtained from Polymer Source, Inc., in 1.5% toluene solution to spin-coat PS-*b*-PMMA films ∼30 nm thick at 4000 rpm spin speed onto silicon nitride substrates. The substrates had been previously cleaned using ultrasonication in toluene, acetone, and methanol for a total of 30 min. Some of the samples were then preannealed in an ultrapure argon atmosphere at 518 K for 12 h. All samples were heated in the oxygen-free high-temperature closed cell of Asylum Research's MFP-3D AFM. Typical scan sizes varied between 0.5 and 2 μm, with time per frame between 30 and 180 s. This corresponded to tip speeds of 4−12 μm/s with higher scan speeds tending to cause slight distortion of parts of the image. Imaging was performed in AC (tapping) mode, using Olympus AC160TS cantilevers with a spring constant of ∼42 N/m and at set point values of 70−90% of free air amplitude. While a range of scanning conditions can yield high-quality diblock images, these particular conditions were chosen to allow continuous imaging at high temperatures for tens of hours. At these conditions, PMMA domains appeared white in topography, as in the literature,[9] and black in the phase images. Note, however, that the contrast in the phase images depends on the AFM imaging parameters. By comparing the phase and the height images, we can identify PMMA domains as black in phase.

The samples were mounted directly onto the heater in order to maximize thermal contact between the sample and the heater as well as minimize drift due to thermal expansion of an adhesive. Imaging was performed between 300 and 520 K in a closed cell under room-temperature argon flow. The glass transition temperature T_g for the constituent blocks of PS-*b*-PMMA is 373−378 K.[9] Differential scanning calorimetry measurements put the bulk T_g for this diblock at 383 K.[10] When changing temperature, samples were heated at the rate of 1−5 K/min. The images were combined to make drift-corrected movies using built-in MFP-3D FFT-based procedure.

Image processing was performed using Image J processing software, available from the NIH Web site,[25] to identify and study polymer domains. During multiple-hour scans, the AFM free air amplitude tends to drift; hence, the gray levels are not the same for all the images. We applied a built-in Image J routine to normalize all of the histograms in a given image sequence.

* Corresponding author. E-mail s-sibener@uchicago.edu.
[†] James Franck Institute and Department of Physics, University of Chicago.
[‡] Asylum Research Corporation.
[§] James Franck Institute and Department of Chemistry, University of Chicago.

10.1021/ma802751c CCC: $40.75
Published on Web 03/09/2009

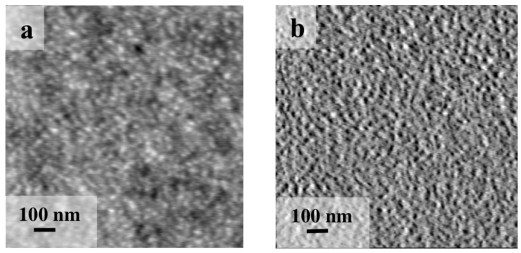

Figure 1. AFM height (a) and phase (b) images of PS-*b*-PMMA at 373 K *without* a prior anneal. PMMA domains appear in white in the height image, as they are raised compared to the matrix, and in black in the phase.

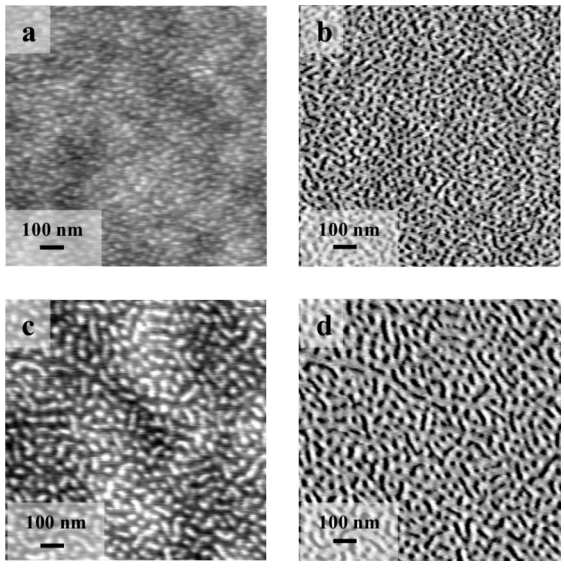

Figure 2. AFM height (a, c) and their corresponding phase (b, d) images of PS-*b*-PMMA at 398 K, *without* a prior high-temperature anneal. The images were taken 8 min apart, the first image being taken within 5 min of reaching that temperature. The ramp rate was 20 K/min. The average interdomain spacing is 35 nm in (a, b) and 40 nm in (c, d).

We then used another standard Image J command—automatic thresholding—to subtract off the background. Finally, we employed the particle measuring routine to study the number, location, and area of domains.

Results and Discussion

1. Formation of Domains. We find that at room temperature, without any annealing, the films consist of disordered micelles of PMMA in a matrix of PS, as observed in prior experiments.[26] This morphology persists for temperatures up to and including T_g, for short and medium heating times—minutes to hours—as shown in Figure 1. Within 15 min of reaching 398 K, there is a transition which turns micelles into rudimentary cylinders, as evidenced by the appearance of significantly longer domains as well as an increase in domain spacing: 40 nm instead of 35 nm, as seen in Figure 2. To our knowledge, this is the first time this transition was observed in situ in real space and not in Fourier space, as in the earlier work by Bates and co-workers which showed polymer stretching well below the order-disorder transition via neutron scattering.[27] The domains of PMMA vary between 12 and 100 nm in length, with an average domain length of 50 nm. Short and long domains are interspersed: there is no particular region where order is nucleated.

According to Binder,[28] the energy barrier for nucleation in asymmetric diblock copolymers grows as $N^{1/2}|f - 0.5|^5 k_B T$, where N is the degree of polymerization, f is the volume fraction of one of the blocks, and T is the temperature. Substituting in the values for N and f for our particular polymer, i.e., $N = 700$ and $f = 0.7$, we obtain a nucleation barrier of $\sim 0.01\ k_B T$, consistent with the observation that microphase separation happens everywhere at once in our experiment.

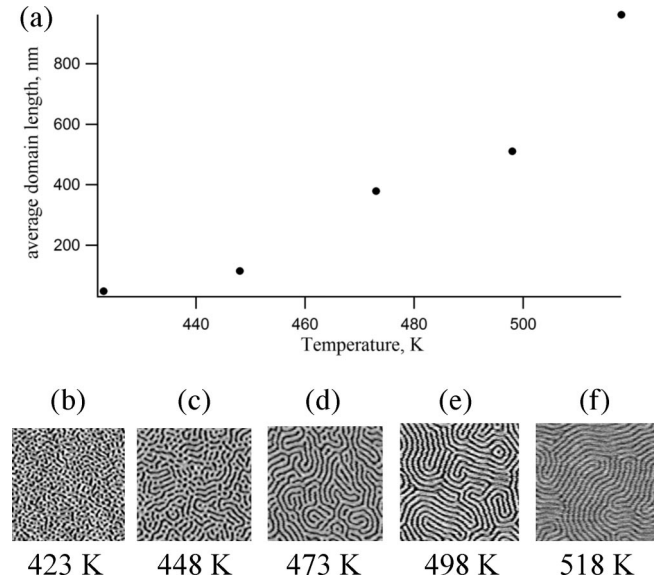

Figure 3. (a) Average length of PMMA domains as a function of temperature. The data were taken at earliest possible times, within minutes of reaching a particular temperature. Ramp rates of 20 K/min were used. Parts b—f show the $1 \times 1\ \mu m^2$ AFM images from which the average domain length was calculated.

2. Growth of Microdomains at Early Times. It is known that the growth of microdomains at a fixed temperature proceeds as a power law as a function of time, i.e., average microdomain length grows as $C(T)t^{0.25}$, where $C(T)$ is a prefactor independent of time.[29,30] Time-lapse AFM studies of disclination and dislocation dynamics provide critical insights into the spatial—temporal evolution of such domains.[30,31] Until now, there have been little data on $C(T)$. In Figure 3, we show our measurements of $C(T)$/10 min, i.e., the average domain length for five distinct temperatures after 10 min.

To obtain measurements of average microdomain length, we first found the number of microdomains in a given square image and their total area. The microdomain number density varied between 500 and 36 per square micron for the temperature range between 423 and 518 K. The images used in this calculation are shown in Figure 3b—f. We then divided the total area occupied by the microdomains by their number times the average width of a domain to get their approximate average length, plotted in Figure 3a. For a linear fit, the slope of the length versus temperature curve is 9 nm/K. This result has practical implications for polymer processing—it means that for every degree increase in annealing temperature, the average microdomain length grows by 9 nm within minutes.

3. Joints and Separations of Microdomains. As Magerle and colleagues have shown with poly(styrene-*block*-butadiene), high-temperature AFM studies of diblock copolymer domains joining and breaking up are feasible.[16] Since PS-*b*-PMMA has a significantly higher T_g than PS-*b*-PB, and our closed cell allowed for imaging up to 570 K, we were able to image both below and above T_g. Consequently, we were able to study in more detail the effect of temperature on domain wall fluctuations, which were responsible for domain joints and breakups. Figure 4 shows an image sequence of microdomains joining.

By imaging the same location continuously for 15 h at 423 K at the rate of 3 min per frame, we find that there exist pairs of open-ended cylinders which never connect with each other

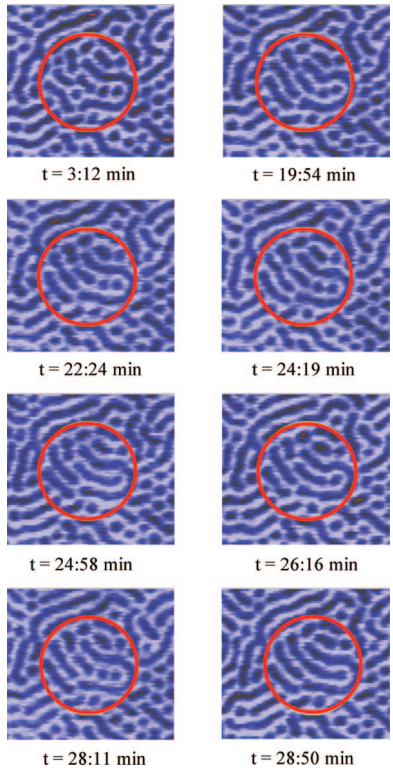

Figure 4. AFM images of PMMA domains joining and breaking up at a fixed temperature (448 K). In the circled region, four separate domains join into one via a series of joints and breaks. The images are 500 × 450 nm^2.

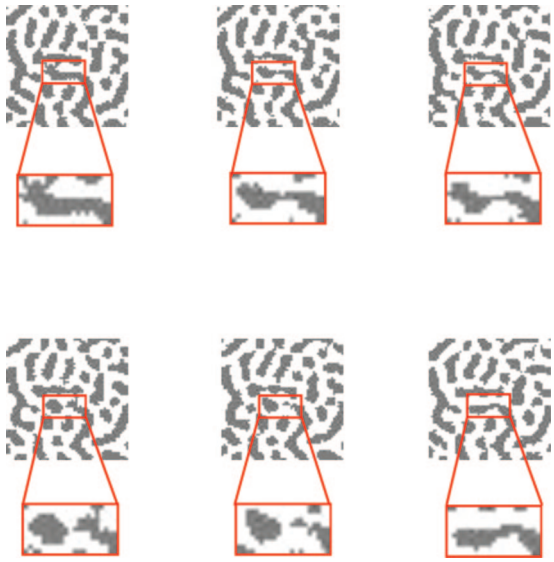

Figure 5. AFM images of a 200 × 200 nm^2 PMMA/PS boundary. The images were taken 30 s apart and show that protrusions of the PMMA (black) domain are followed by retractions, indicating that there is a restoring force. Since the force is isotropic, it cannot be due to some larger scale flows. Curvature minimization is thus the likeliest force responsible.

and, at the other extreme, those which join and break up every 10 min, on average. We identify this frequency with the rate at which the cylinders attempt to connect or break apart. Now we can obtain the activation energy for this transition by using the Boltzmann distribution $p = e^{-E/k_BT}$, where p is the probability of a transition and E_A is activation energy. The probability of a transition is the number of successful transitions divided by the number of attempted ones.

We consider pairs of open-ended microdomains which, over the course of 15 h (300 images), do join or break up, i.e., "switch". By analyzing 300 sequential images of ~1 μm^2 area, we find that for a few typical pairs of domains switches occur 22, 32, 40, 53, 71, 88, 100, and 106 times. Future studies will determine the reasons for such a widespread in values—the distribution of PS and PMMA segments on the surface and inside the film, the local geometry of the domains, or other factors.

An example of a microdomain switching several times is shown in Figure 4. We note that, on average, a pair of domains has a probability of switching equal to the total number of switches divided by the total possible number of switches for the eight pairs: $512/(300 \times 8) = 0.2 \pm 0.1$.

Given that the probability of switching varies between 0.1 and 0.3 from above, it follows from the Boltzmann distribution that the activation energy for two cylindrical microdomains joining/breaking up is thus between 0.3 and 1.4 k_BT, which is equivalent to 0.01−0.06 eV. This range agrees with the finding of Magerle and colleagues for the activation energy in the cylindrical PS-*b*-PB system of 0.4 k_BT.[16]

Previously, only a single temperature was accessible for observing domain switching in situ using AFM.[16] From AFM movies (see Supporting Information) we have observed that domain switching becomes more frequent as a function of temperature, suggesting that activation energy for this process is constant. Further studies are necessary to confirm this finding.

4. Fluctuations. As mentioned in the Introduction, the main theories for polymer chain motion are large-scale flows,[21] domain curvature minimization,[22] tubelike reptation,[23] and Rousian diffusion.[24] By compiling our AFM data into time-lapse movies, we have been able to observe how small-scale fluctuations result in domain joints and separations.

Since our images offer high resolution, we are able to resolve nanometer-scale fluctuations present perpendicular to the interdomain divide, as shown in Figure 6. A natural question is whether the fluctuations observed are real or a result of imaging noise. If one believes the dramatic changes observed, such as microdomains fully joining or breaking apart, it seems difficult to claim that smaller fluctuations which often precede such events are simply imaging noise.

Because we see oscillations and not simple diffusion on this scale, we can conclude that there exists a restoring force which returns the chains back into domains. Moreover, since the oscillations are occurring perpendicular to the microdomain boundary, a reptation-like mechanism must be responsible for producing them. This is because ordinary Rousian diffusion, which is a Brownian chain representing the polymer, would have a high energy cost associated with the chain crossing the interdomain boundary, whereas for reptation, this energy cost is small.[24]

What is the restoring force responsible for pulling the chains back into the microdomains? It seems that large-scale flows are ruled out, as they would imply that on the scale of hundreds of nanometers, all ordering would proceed along a single direction, which is not the case in our images. Moreover, our films were prepared within a nanometer of equilibrium monolayer thickness and hence did not have significant large-scale flows corresponding to formation of islands and holes. Rousian diffusion is ruled out also, as it would most likely lead to motion along the interdomain dividing surface, not perpendicular to it. Tube-like reptation alone would lead to chains continually moving away from their starting points, and hence a restoring force is required to explain our observations. We therefore hypothesize that the likely force is domain curvature minimization. We have observed in the movies that every nanometer-scale protrusion

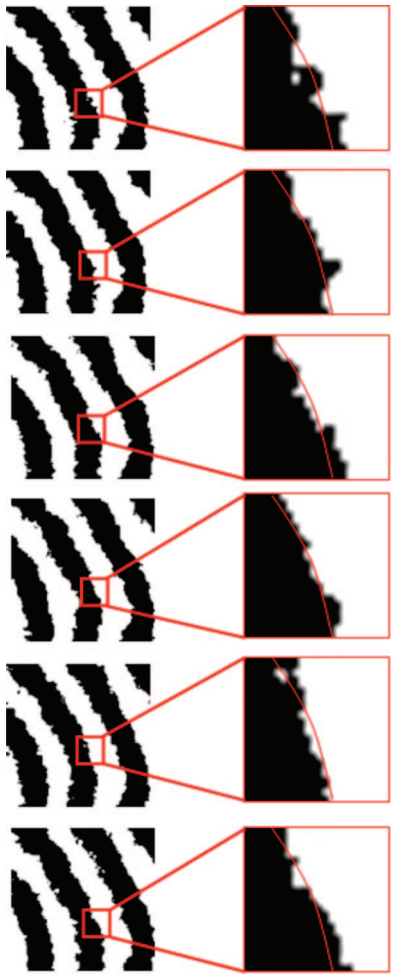

Figure 6. AFM images of a 100 × 100 nm^2, with a 10 × 10 nm^2 region magnified, showing the PMMA/PS boundary. The images were taken 30 s apart and show that protrusions of the PMMA (black) domain are followed by retractions, indicating that there is a restoring force. Since the force is isotropic, it cannot be due to some larger scale flows. Curvature minimization is thus the likeliest force responsible.

of PMMA which increases local interdomain curvature significantly is followed by a withdrawal which reduces the curvature, as shown in Figure 6.

We have measured the spatiotemporal correlation function at a range of temperatures to gain a quantitative understanding of the temperature dependence of the fluctuations. This correlation function was defined as the fractional overlap between the PMMA domains in a given area considered at earlier and later times. We find that, on the scale of minutes and even hours, the system has a built-in memory, and the overlap of the pattern at some initial time and a later time is large (see Figure 7), although domain boundaries are fluctuating, as shown above. Representative movies taken at 373, 413, and 453 K can be found in the Supporting Information.

We have also observed the motion of the center of mass of similar microdomains for a range of temperatures. We picked circular microdomains, since at every temperature our sequence of AFM images was taken we could easily identify such domains, as shown in Figure 8a. We measured the distances by which these domains moved in 30 s intervals, i.e., between frames, as given by their center-of-mass positions. In diffusion, a particle's distance traveled is proportional to the square root of the diffusion constant times time. Since we take the time interval for all cases to be the same, we can disregard the time dependence in this case. Moreover, according to the Einstein

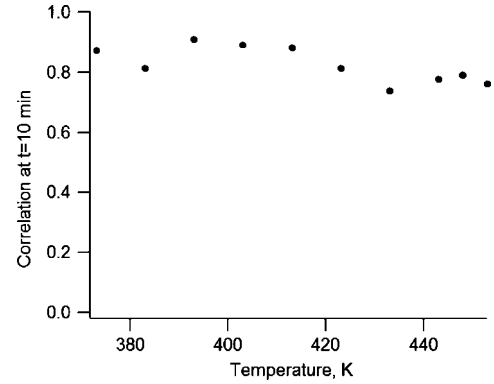

Figure 7. Overlap of PMMA domains at $t = 0$ and $t = 10$ min, normalized by the average fraction of the area covered at each time, measured as a function of temperature. The overlap between the earlier and later times is at least 80% between 373 and 453 K; i.e., domains are mostly staying in place on the time scale of 10 min, while their edges are fluctuating. (Overall instrumental drift has been subtracted off.)

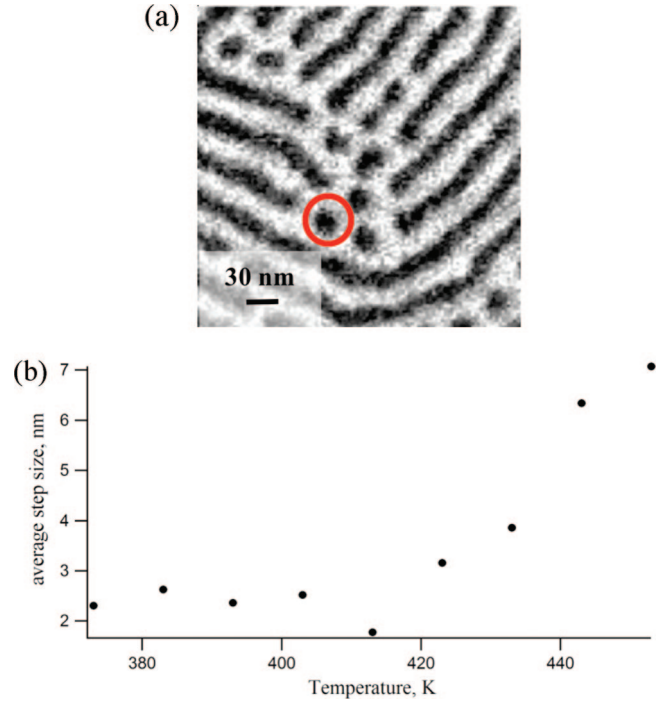

Figure 8. (a) AFM image exhibiting circular domains, with one such domain circled. (b) Twenty-frame averages of distance traveled between frames for circular domains, $|\Delta r_{cm}|$. Note the transition which happens around 420 K: $|\Delta r_{cm}|$ is roughly constant below 420 K and is within the 2−3 nm measurement error and grows linearly with temperature above 420 K.

relation, the diffusion constant is linear with respect to temperature. Thus, if the domains move via diffusion, we expect the distance traveled between frames to grow as a square root of temperature if the viscosity of the medium does not change significantly.

We found that, consistent with qualitative observations from the movies, there is a qualitative shift in the motion of domains at 413 K. Below this temperature, the average distance traveled was constant as a function of temperature and was within the estimated registration error between subsequent movie frames of 2−3 nm. Above 413 K, it grew approximately linearly with temperature, as shown in Figure 8b. One likely explanation is

that the viscosity of the polymer is changing significantly with temperature.

Summary

We have observed in situ polymer microdomain formation and evolution directly, using AFM imaging with environmental control. As temperature was increased through the glass transition, micelles became cylindrical microdomains everywhere at temperatures of 398 K and above within minutes. We also found that, upon initial heating above T_g, quasi-equilibrium patterns were established within minutes of reaching a particular temperature. Subsequent isothermal microdomain growth proceeded very slowly, suggesting that higher temperatures (significantly above T_g but below T_{ODT}) led to faster ordering for this diblock.

By imaging the same area over the course of hours, we have been able to observe thousands of domain separations and joints. By comparing the number of successful joints and separations to the number of attempts, we obtained a value for the energy of activation. We also observed oscillations perpendicular to the interdomain surface and not parallel to it. This implies that a reptation-like mechanism, combined with curvature minimization, was most likely responsible for individual chain motion.

Acknowledgment. We thank Tom Witten and Ward Lopes for useful discussions. This work was supported by the Army Research Office/DTRA and by U of C MRSEC Grants NSF-DMR-0213745 and NSF-DMR-0820054.

Supporting Information Available: AFM time-lapse movies taken at 373, 413, and 453 K. This material is available free of charge via the Internet at http://pubs.acs.org.

References and Notes

(1) Fredrickson, G. H.; Bates, F. S. *Annu. Rev. Mater. Sci.* **1996**, *26*, 501–550.
(2) Bockstaller, M. R.; Mickewicz, R. A.; Thomas, E. L. *Adv. Mater.* **2005**, *17*, 1331–1339.
(3) Black, C. T.; Ruiz, R.; Breyta, G.; Cheng, J. Y.; Colburn, M. E.; Guarini, K. W.; Kim, H.-C.; Zhang, Y. *IBM J. Res. Dev.* **2007**, *51*, 605–633.
(4) Hamley, I. W. *Nanotechnology* **2003**, *14*, R39–R54.
(5) Darling, S. B. *Prog. Polym. Sci.* **2007**, *32*, 1152–1204.
(6) Sundrani, D.; Darling, S. B.; Sibener, S. J. *Nano Lett.* **2004**, *4*, 273. 000Sundrani, D.; Darling, S. B.; Sibener, S. J. *Langmuir* **2004**, *20*, 5091–5099.
(7) Segalman, R. A. *Mater. Sci. Eng. R* **2005**, *48*, 191–226.
(8) Naito, K.; Hieda, H.; Sakurai, M.; Kamata, Y.; Asakawa, K. *IEEE Trans. Magn.* **2002**, *38*, 1949–1951.
(9) Hahm, J.; Lopes, W. A.; Jaeger, H. M.; Sibener, S. J. *J. Chem. Phys.* **1998**, *109*, 10111–10114.
(10) Polymer Source, Quebec H9P 2X8, Canada.
(11) Quiram, D.; Register, R. A.; Marchand, G. R. *Macromolecules* **1997**, *30*, 4551–4558.
(12) Li, W.; Sheller, N.; Foster, M. D.; Baralishis, D.; Manners, I.; Annis, B.; Lin, J. S. *Polymer* **2000**, *41*, 719–724.
(13) Liu, Z.; Shaw, M.; Hsiao, B. *Macromolecules* **2004**, *37*, 9880–9888.
(14) Singh, M. A.; Harkless, C. R.; Nagler, S. E.; Shannon, R. F.; Ghosh, S. S. *Phys. Rev. B* **1993**, *47*, 8425–8435.
(15) Grim, P. C. M.; Nyrkova, I. A.; Semenov, A. N.; ten Brinke, G.; Hadziioannou, G. *Macromolecules* **1995**, *28*, 7501–7513.
(16) Tsarkova, L.; Knoll, A.; Magerle, R. *Nano Lett.* **2006**, *6*, 1574–1577.
(17) McLeish, T. C. B. *Adv. Phys.* **2002**, *51*, 1379–1527.
(18) Morkved, T. L.; Jaeger, H. M. *Europhys. Lett.* **1997**, *40*, 643–648.
(19) Graessley, W. *Adv. Polym. Sci.* **1982**, *47*, 67–112.
(20) Horvat, A.; Knoll, A.; Krausch, G.; Tsarkova, L.; Lyakhova, K. S.; Sevink, G. J. A.; Zvelindovsky, A. V.; Magerle, R. *Macromolecules* **2007**, *40*, 6930–6939.
(21) Fredrickson, G. H. *J. Rheol.* **1994**, *38*, 1045–1067.
(22) Thomas, E. L.; Lescanec, R. L. *Philos. Trans. R. Soc. London A* **1994 34**, *8*, 149000.
(23) Pokrovskii, V. N. *Physica A* **2006**, *366*, 88–106.
(24) Doi, M.; Edwards, S. F. *The Theory of Polymer Dynamics*; Oxford University Press: New York, 1986.
(25) Image J is available free of charge at http://rsbweb.nih.gov/ij/.
(26) Khaydarov, A. A.; Hamley, I. W.; Legge, T. M.; Perrier, S. *Eur. Polym. J.* **2007**, *43*, 789–796.
(27) Almdal, K.; Rosedale, J. H.; Bates, F. S.; Wignall, G. D.; Fredrickson, G. H. *Phys. Rev. Lett.* **1990**, *65*, 1112–1115.
(28) Binder, K. *Physica A* **1995**, *213*, 118–129.
(29) Harrison, C.; Adamson, D. H.; Cheng, Z.; Sebastian, J. M.; Sethuraman, S.; Huse, D. A.; Register, R. A.; Chaikin, P. M. *Science* **2000**, *290*, 1558–1560.
(30) Harrison, C.; Cheng, Z.; Sethuraman, S.; Huse, D. A.; Chaikin, P. M. *Phys. Rev. E* **2002**, *66*, 011706/1-27.
(31) Hahm, J.; Sibener, S. J. *J. Chem. Phys.* **2001**, *114*, 4730–4740.

MA802751C